2018 IEEE 7th Data Driven Control and Learning Systems Conference
May 25-27, 2018, Enshi, Hubei Province, China

Saturated D-type ILC for Multicopter Trajectory Tracking Based on Additive State Decomposition

Chenxu Ke, Jinrui Ren, Quan Quan
School of Automation Science and Electrical Engineering, Beihang University, Beijing 100191, P. R. China
E-mail: ke_chenxu@buaa.edu.cn;renjinrui@buaa.edu.cn;qq_buaa@buaa.edu.cn

Abstract: In this paper, a saturated D-type iterative learning control (ILC) method is proposed for multicopter trajectory tracking based on the additive state decomposition (ASD) method. By using the ASD method, the multicopter nonlinear horizontal channel with input saturation is divided into a linear primary system and a nonlinear secondary system. The ILC method for linear systems can be used directly in the linear primary system to track desired trajectories. A state feedback is applied to stabilize the nonlinear secondary system. Then, the above two controllers are combined to achieve the control goal. Simulation results demonstrate the feasibility of the proposed method for the multicopter trajectory tracking problem with input saturation and other nonlinearities.

Key Words: Multicopter, Iterative Learning Control, Additive State Decomposition, Trajectory Tracking

1 Introduction

Trajectory tracking is an important application for multicopters. Stability, robustness, and maneuverability are essential requirements for the multicopters in trajectory tracking tasks. In trajectory tracking tasks, multicopters may need to execute missions, repetitively. For example, takeoff and landing of multicopters are repetitive processes in flying tasks. In different tasks and situations, there are many disturbances. The iterative learning control (ILC) method can be applied to multicopters to achieve trajectory tracking goals by rejecting disturbances and reducing tracking errors [1]. The ILC method has been applied to industrial robots [2], autonomous vehicles [3] and other industrial fields to reject repetitive disturbances. By applying the ILC method to multicopters, multicopters' stability, robustness, and maneuverability can be improved efficiently [4]. In short, the ILC method is appropriate for the multicopter repetitive trajectory tracking problem.

In practice, the inputs of the multicopter horizontal channel are often required to be small. One reason is to decouple the multicopter horizontal channel model. Another reason is that the ILC method without input saturation may cause an unaccepted iterative transient process, although a convergent result can be obtained [5]. Thus, in general, the multicopter horizontal channel is regarded as a nonlinear system with input saturation. For nonlinear problems, an additive-state-decomposition (ASD) method is proposed in references [6, 7] to simplify the controller design. Concretely, the nonlinear original system is divided into two subsystems including a linear system called *primary* system and a nonlinear system called *secondary* system. Then, two controllers for the two subsystems are designed, respectively, by using existing methods. With the secondary system being stabilized by using state feedback, linear system control laws can be used for the primary system to achieve the control goal of the original system. Comparing with linearization [9] and partial linearization [**?**], the ASD method does not neglect nonlinearities.

This work was supported by National Natural Science Foundation of China (No. 61473012).

For the multicopter horizontal channel model, a saturated ILC method based on ASD is given to solve the multicopter horizontal channel nonlinear trajectory tracking problem in this paper. First, the horizontal channel model, namely the original system, is given. Then, by applying the ASD method, two subsystems including a linear primary system and a nonlinear secondary system are obtained. For the two subsystems, two independent controllers and an observer are designed. For simplicity, a D-type ILC method is used for the linear primary system. Since the output matrix of the primary system does not satisfy the convergence condition of the D-type ILC method, the velocity of multicopters are added to the position of multicopters giving a new output. A state feedback is applied for the stabilization of the secondary system. Then, the convergence results of the two subsystems under their controllers are proved. Finally, simulation results show the feasibility and effectiveness of the method mentioned above.

As mentioned above, three contributions of this paper to the multicopter trajectory tracking problem are as follows:

- Modifying the output matrix of the primary system to satisfy the convergence condition of the D-type ILC method.
- Through the ASD method, many linear control laws can be used by the linear primary system to achieve trajectory tracking goals flexibly. What is more, under the ASD framework, better results can be obtained. For example, reference [10] proposed an adjoint-type ILC method based on ASD to solve the nonlinear system tracking problem.
- The nonlinear secondary system can be stabilized by state feedback rather than complex control methods. Ignoring nonlinearities by linearization or partial linearization of nonlinear systems may decrease the convergence rate. However, this is avoided by the ASD method.

The structure of this paper is as follows. The multicopter horizontal channel model is given in the Section 2. In Section 3, the integrated controller including a D-type ILC controller, a state feedback controller, and an observer is constructed. Simulation results with analyses are provided in

Section 4. Then, in section 5, the conclusion is given .

2 Problem Formulation

In this section, the multicopter horizontal position channel model is extracted from the multicopter rigid body position and velocity model.

The multicopter rigid body position and velocity model is expressed as follows:

$$\begin{cases} \dot{\mathbf{p}} = \mathbf{v} \\ \dot{\mathbf{v}} = g\mathbf{e}_3 - \dfrac{f}{m}\mathbf{R}\mathbf{e}_3 \end{cases} \tag{1}$$

where $\mathbf{p} = \begin{bmatrix} p_x & p_y & p_z \end{bmatrix}^{\mathrm{T}} \in \mathbb{R}^3$ is the position of the Center of Gravity (CoG) of the multicopter, $\mathbf{v} = \begin{bmatrix} v_x & v_y & v_z \end{bmatrix}^{\mathrm{T}} \in \mathbb{R}^3$ is the multicopter velocity, g represents the value of the acceleration of gravity, $\mathbf{e}_3 = \begin{bmatrix} 0 & 0 & 1 \end{bmatrix}^{\mathrm{T}}$, f represents the propeller thrust, m is the mass of the multicopter, $\mathbf{R}$ denotes a rotation matrix from the Earth-Fixed Coordinate Frame (EFCF) to the Aircraft-Body Coordinate Frame (ABCF), and its definition is

$$\mathbf{R} = \begin{bmatrix} \mathbf{r}_1 & \mathbf{r}_2 & \mathbf{r}_3 \end{bmatrix} \tag{2}$$

where

$$\mathbf{r}_1 = \begin{bmatrix} \cos\theta\cos\psi \\ \cos\theta\sin\psi \\ -\sin\theta \end{bmatrix}$$

$$\mathbf{r}_2 = \begin{bmatrix} \cos\psi\sin\theta\sin\phi - \sin\psi\cos\phi \\ \sin\psi\sin\theta\sin\phi + \cos\psi\cos\phi \\ \sin\phi\cos\theta \end{bmatrix}$$

$$\mathbf{r}_3 = \begin{bmatrix} \cos\psi\sin\theta\cos\phi + \sin\psi\sin\phi \\ \sin\psi\sin\theta\cos\phi - \cos\psi\sin\phi \\ \cos\phi\cos\theta \end{bmatrix}$$

with $\theta, \phi, \psi \in \mathbb{R}$ denoting the pitch angle, roll angle and yaw angle, respectively.

Suppose that the multicopter does not perform large angle maneuvering, an assumption is given to simplify the multicopter horizontal channel model.

Assumption 1. The total thrust approximates to the weight of the multicopter, that is $f \approx mg$.

According to *Assumption 1* and considering input saturation, the multicopter horizontal channel model is given as follows:

$$\begin{cases} \dot{\mathbf{p}}_{\mathrm{h}} = \mathbf{v}_{\mathrm{h}} \\ \dot{\mathbf{v}}_{\mathrm{h}} = -g\mathbf{G}_{\mathrm{h}\psi}(\mathrm{sat}(\mathbf{u})) \end{cases} \tag{3}$$

where

$$\mathrm{sat}(\mathbf{u}) = \begin{bmatrix} \mathrm{sat}(\theta) \\ \mathrm{sat}(\phi) \end{bmatrix}, \mathbf{p}_{\mathrm{h}} = \begin{bmatrix} p_x \\ p_y \end{bmatrix}, \mathbf{v}_{\mathrm{h}} = \begin{bmatrix} v_x \\ v_y \end{bmatrix}$$

$$\mathbf{G}_{\mathrm{h}\psi}(\mathrm{sat}(\mathbf{u})) =$$

$$\begin{bmatrix} \cos\psi\sin(\mathrm{sat}(\theta))\cos(\mathrm{sat}(\phi)) + \sin\psi\sin(\mathrm{sat}(\phi)) \\ \sin\psi\sin(\mathrm{sat}(\theta))\cos(\mathrm{sat}(\phi)) - \cos\psi\sin(\mathrm{sat}(\phi)) \end{bmatrix}$$

for each element of the vector $\mathbf{u}$, define the saturation function $\mathrm{sat}(\cdot)$ as follows:

$$\mathrm{sat}(u) = \begin{cases} u_{\min}, & u < u_{\min} \\ u, & u_{\min} \le u < u_{\max} \\ u_{\max}, & u_{\max} \le u \end{cases} \tag{4}$$

Defining the multicopter's position as output, that is $\mathbf{y} = \mathbf{p}_{\mathrm{h}}$, the multicopter horizontal channel system with input saturation can be rewritten as

$$\text{Original system:} \begin{cases} \dot{\mathbf{x}} = \mathbf{A}\mathbf{x} - g\mathbf{G}_{\psi}(\mathrm{sat}(\mathbf{u})) \\ \mathbf{y} = \mathbf{C}\mathbf{x}, \mathbf{x}(0) = \mathbf{0} \end{cases} \tag{5}$$

where

$$\mathbf{u} = \begin{bmatrix} \theta \\ \phi \end{bmatrix}, \mathbf{x} = \begin{bmatrix} \mathbf{p}_{\mathrm{h}} \\ \mathbf{v}_{\mathrm{h}} \end{bmatrix}$$

$$\mathbf{A} = \begin{bmatrix} 0 & 0 & 1 & 0 \\ 0 & 0 & 0 & 1 \\ 0 & 0 & 0 & 0 \\ 0 & 0 & 0 & 0 \end{bmatrix}$$

$$\mathbf{C} = \begin{bmatrix} 1 & 0 & 0 & 0 \\ 0 & 1 & 0 & 0 \end{bmatrix}$$

$$\mathbf{G}_{\psi}(\mathrm{sat}(\mathbf{u})) =$$

$$\begin{bmatrix} 0 \\ 0 \\ \cos\psi\sin(\mathrm{sat}(\theta))\cos(\mathrm{sat}(\phi)) + \sin\psi\sin(\mathrm{sat}(\phi)) \\ \sin\psi\sin(\mathrm{sat}(\theta))\cos(\mathrm{sat}(\phi)) - \cos\psi\sin(\mathrm{sat}(\phi)) \end{bmatrix}$$

Considering the input saturation and small angle maneuvering, another assumption is stated as follows.

Assumption 2. The roll angle and pitch angle are small [11, p.255], that is $\sin\phi \approx \phi, \cos\phi \approx 1, \sin\theta \approx \theta, \cos\theta \approx 1$.

According to *Assumption 2*, one has

$$\begin{aligned} \mathbf{G}_{\psi}(\mathrm{sat}(\mathbf{u})) &\approx \begin{bmatrix} 0 \\ 0 \\ \cos\psi\mathrm{sat}(\theta) + \sin\psi\mathrm{sat}(\phi) \\ \sin\psi\mathrm{sat}(\theta) - \cos\psi\mathrm{sat}(\phi) \end{bmatrix} \\ &= \mathbf{B}_{\psi}\mathrm{sat}(\mathbf{u}) \end{aligned} \tag{6}$$

where

$$\mathbf{B}_{\psi} = \begin{bmatrix} 0 & 0 \\ 0 & 0 \\ \cos\psi & \sin\psi \\ \sin\psi & -\cos\psi \end{bmatrix}.$$

Remark 1. If $\mathbf{x}(0) \neq \mathbf{0}$, it can be transformed to $\mathbf{x}(0) = \mathbf{0}$ by using the methods mentioned in [12] or [13].

3 ASD-Based ILC Framework

In this section, the original system (5) is decomposed into two systems by using the ASD method. One is a linear primary system, and the other is a saturated secondary system which is a nonlinear system. Since the observer for the states of the secondary system and the primary system outputs can be constructed, the original system trajectory tracking problem can be transformed into an linear system trajectory tracking problem and a nonlinear system stabilization problem.

3.1 Additive State Decomposition

Applying ASD to system (5) and considering equation (6), the primary system is chosen as

$$\begin{cases} \dot{\mathbf{x}}_{\mathrm{p}} = \mathbf{A}\mathbf{x}_{\mathrm{p}} - g\mathbf{B}_{\psi}\mathbf{u}_{\mathrm{p}} \\ \mathbf{y}_{\mathrm{p}} = \mathbf{C}\mathbf{x}_{\mathrm{p}}, \mathbf{x}_{\mathrm{p}}(0) = \mathbf{0} \end{cases} \tag{7}$$

where

$$\mathbf{u}_{\mathrm{p}} = \begin{bmatrix} \theta_{\mathrm{p}} \\ \phi_{\mathrm{p}} \end{bmatrix}, \mathbf{x}_{\mathrm{p}} = \begin{bmatrix} \mathbf{p}_{\mathrm{hp}} \\ \mathbf{v}_{\mathrm{hp}} \end{bmatrix}, \mathbf{y}_{\mathrm{p}} = \mathbf{p}_{\mathrm{hp}}$$

In practice, the yaw angle ψ is mostly constant. Thus $\mathbf{B}_{\psi}$ is constant. Then, the primary system (7) becomes an LTI system. By subtracting system (7) from system (5), one has

$$\begin{cases} \dot{\mathbf{x}} - \dot{\mathbf{x}}_{\mathrm{p}} = \mathbf{A}(\mathbf{x} - \mathbf{x}_{\mathrm{p}}) - (g\mathbf{G}_{\psi}(\mathrm{sat}(\mathbf{u})) - g\mathbf{B}_{\psi}\mathbf{u}_{\mathrm{p}}) \\ \mathbf{y} - \mathbf{y}_{\mathrm{p}} = \mathbf{C}(\mathbf{x} - \mathbf{x}_{\mathrm{p}}), \mathbf{x}(0) - \mathbf{x}_{\mathrm{p}}(0) = \mathbf{0}. \end{cases} \tag{8}$$

Then, by defining

$$\mathbf{u}_{\mathrm{s}} = \mathbf{u} - \mathbf{u}_{\mathrm{p}} = \begin{bmatrix} \theta_{\mathrm{s}} \\ \phi_{\mathrm{s}} \end{bmatrix}$$
$$\mathbf{x}_{\mathrm{s}} = \mathbf{x} - \mathbf{x}_{\mathrm{p}} = \begin{bmatrix} \mathbf{p}_{\mathrm{hs}} \\ \mathbf{v}_{\mathrm{hs}} \end{bmatrix}$$
$$\mathbf{y}_{\mathrm{s}} = \mathbf{y} - \mathbf{y}_{\mathrm{p}} = \mathbf{p}_{\mathrm{hs}}$$

system (8) becomes the secondary system as follows:

$$\begin{cases} \dot{\mathbf{x}}_{\mathrm{s}} = \mathbf{A}\mathbf{x}_{\mathrm{s}} - g\mathbf{G}_{\psi}(\mathrm{sat}(\mathbf{u})) + g\mathbf{B}_{\psi}\mathbf{u}_{\mathrm{p}} \\ \mathbf{y}_{\mathrm{s}} = \mathbf{C}\mathbf{x}_{\mathrm{s}}, \mathbf{x}_{\mathrm{s}}(0) = \mathbf{0} \end{cases} \tag{9}$$

which is a nonlinear system.

Above all, the original system (5) is divided into a linear primary system (7) and a nonlinear secondary system (9) with a nonlinear term.

Before the decomposition of the original system (5), the control objective is as follows:

Objective: Construct a control sequence $\mathbf{u}(t) = \mathbf{u}_k(t)$ for system (5), such that

$$\|\mathbf{y}_{\mathrm{d}} - \mathbf{y}_k\|_{[0,T]} \to 0, \text{as } k \to \infty$$

where $\mathbf{y}_{\mathrm{d}}$ is the desired trajectory, $\mathbf{y}_k$ is the output of system (5) driven by $\mathbf{u}_k$, k denotes the iteration number, $k = 1, 2, 3, \ldots$, and $\mathbf{u}_1(t) = \mathbf{0}$, $t \in [0, T]$.

After the decomposition of the original system (5), the control objective is also divided as shown in Fig. 1. For the primary system input $\mathbf{u}_{\mathrm{p}}$, the last iteration errors are used to improve the current iteration control sequence. For the secondary system input $\mathbf{u}_{\mathrm{s}}$, state feedback is used.

3.2 Controller Design for Two Subsystems

In this subsection, two controllers are designed to solve the two problems as mentioned before. Note that the original system output is redefined to satisfy the convergence condition of the primary system with ILC controller.

Problem 1 (on the primary system): For system (7), design a D-type ILC input sequence

$$\mathbf{u}_{\mathrm{p},k+1}(t) = \mathbf{u}_{\mathrm{p},k}(t) + \mathbf{\Gamma}_{\mathrm{d}}\dot{\mathbf{e}}_{\mathrm{p},k}(t) \tag{10}$$

to make $\mathbf{e}_{\mathrm{p},k}(t) \to \mathbf{0}$ as $k \to \infty$, where $t \in [0, T]$, T represents the flight time, $\mathbf{\Gamma}_{\mathrm{d}} \in \mathbb{R}^{2\times 2}$ is the gain matrix of the D-type ILC, $\mathbf{e}_{\mathrm{p},k}(t) = \mathbf{y}_{\mathrm{d}}(t) - \mathbf{y}_{\mathrm{p},k}(t)$, $\mathbf{y}_{\mathrm{d}} = \mathbf{v}_{\mathrm{hd}} + \mathbf{p}_{\mathrm{hd}}$.

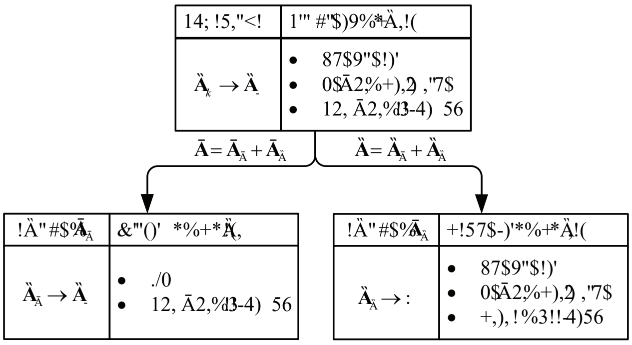

Fig. 1. Additive state decomposition for system (5)

To solve *Problem 1*, the convergence of the primary system (7) under controller (10) the will be proved in the following. *Lemma 1* gives the convergence condition of the LTI system (11) with the D-type ILC controller (12).

Lemma 1[14]. For the LTI system

$$\begin{cases} \dot{\mathbf{x}}_k(t) = \mathbf{A}\mathbf{x}_k(t) + \mathbf{B}\mathbf{u}_k(t) \\ \mathbf{y}_k(t) = \mathbf{C}\mathbf{x}_k(t) \end{cases} \tag{11}$$

design a D-type learning law

$$\mathbf{u}_{k+1}(t) = \mathbf{u}_k(t) + \mathbf{\Gamma}\dot{\mathbf{e}}_k(t) \tag{12}$$

where $t \in [0, T]$, $\mathbf{x}_k(t) \in \mathbb{R}^n, \mathbf{u}_k(t) \in \mathbb{R}^r, \mathbf{y}_k(t) \in \mathbb{R}^m$, $\mathbf{e}_k(t) = \mathbf{y}_{\mathrm{d}}(t) - \mathbf{y}_k(t)$, k represents the iterative number. If

i) $\|\mathbf{I} - \mathbf{\Gamma}\mathbf{C}\mathbf{B}\| < 1$
ii) $\mathbf{x}_k(0) = \mathbf{x}_{\mathrm{d}}(0) \quad (k = 0, 1, 2, \cdots)$.

then, $\mathbf{y}_k(t) - \mathbf{y}_{\mathrm{d}}(t) \to \mathbf{0}$, as $k \to \infty$.

According to *Lemma 1*, the convergence of the primary system (7) with controller (10) is proved.

Theorem 1. For the LTI system (7), if

$$\mathrm{rank}\,(\mathbf{C}\mathbf{B}_{\psi}) = 2 \tag{13}$$

then, $\exists\, \mathbf{\Gamma} \in \mathbb{R}^{2\times 2}$ for the D-type ILC controller (12) makes $\mathbf{e}_k(t) \to \mathbf{0}$ as $k \to \infty$.

Proof. According to *Lemma 1*, for the primary system (7), rank $(\mathbf{C}\mathbf{B}_{\psi}) = 2 \Rightarrow \exists\, \mathbf{\Gamma} \in \mathbb{R}^{2\times 2}$ satisfies the condition i) $\|\mathbf{I} - \mathbf{\Gamma}\mathbf{C}\mathbf{B}_{\psi}\| < 1$. □

Remark 2. Note that in the primary system (7), one has

$$\mathbf{C}\mathbf{B}_{\psi} = \begin{bmatrix} 0 & 0 \\ 0 & 0 \end{bmatrix}$$

and rank$(\mathbf{C}\mathbf{B}_{\psi}) \neq 2$, which do not satisfy the convergence condition. To satisfy the convergence condition (13), according to *Theorem 1*, we redefine

$$\mathbf{y} = \mathbf{p}_{\mathrm{h}} + \mathbf{v}_{\mathrm{h}}$$
$$\mathbf{y}_{\mathrm{p}} = \mathbf{p}_{\mathrm{ph}} + \mathbf{v}_{\mathrm{ph}} = \begin{bmatrix} y_{\mathrm{p}1} \\ y_{\mathrm{p}2} \end{bmatrix}$$
$$\mathbf{y}_{\mathrm{s}} = \mathbf{p}_{\mathrm{sh}} + \mathbf{v}_{\mathrm{sh}} = \begin{bmatrix} y_{\mathrm{s}1} \\ y_{\mathrm{s}2} \end{bmatrix}.$$

Then, the matrix $\mathbf{C}$ is modified to be

$$\begin{bmatrix} 1 & 0 & 1 & 0 \\ 0 & 1 & 0 & 1 \end{bmatrix}.$$

That means that the new outputs of system (5) contain the velocity and the position information of the multicopter.

Based on *Lemma 1* and *Theorem 1*, *Problem 1* is solved by modifying the matrix $\mathbf{C}$. In the following, we are going to study the secondary system.

Problem 2 (on the secondary system): For system (9), design a controller

$$\mathbf{u}_{\mathrm{s},k}(t) = \mathbf{L}^{\mathrm{T}}\mathbf{x}_{\mathrm{s},k}(t) \tag{14}$$

to satisfy that $\|\mathbf{x}_{\mathrm{s},k}\|_{[0,T]} \to 0$ and $\lim\limits_{k\to\infty} \mathbf{y}_{\mathrm{s},k}(t) = \mathbf{0}$, if $\|\mathbf{e}_{\mathrm{p},k}\|_{[0,T]} \to 0$, $\|\tilde{\mathbf{u}}_{\mathrm{p},k}\|_{[0,T]} \to 0$, where $\mathbf{L} \in \mathbb{R}^{2\times 4}$ is a constant matrix.

A solution to *Problem 2* is shown in the following theorem. *Problem 2* will be solved, if *Problem 1* is solved.

Theorem 2. Design the controller $\mathbf{u}_{\mathrm{s}}$ as (14) for the secondary system (9), then, $\mathbf{x}_{\mathrm{s},k} \to \mathbf{0}$, and $\mathbf{y}_{\mathrm{s},k} \to \mathbf{0}$, as $\mathbf{y}_{\mathrm{p},k} - \mathbf{y}_{\mathrm{d}} \to \mathbf{0}$. It means $\lim\limits_{k\to\infty} \mathbf{y}_{\mathrm{s},k}(t) = \mathbf{0}$.

Proof. See *Reference* [10]. □

According to *Theorem 2*, *Problem 2* can be solved using any constant matrix $\mathbf{L}$. However, an inappropriate $\mathbf{L}$ may decrease the convergence rate. For such a purpose, how to choose an appropriate matrix $\mathbf{L}$ is given in [10].

3.3 Integration Design

In this subsection, controllers (10) and (14) are combined and an observer is given.

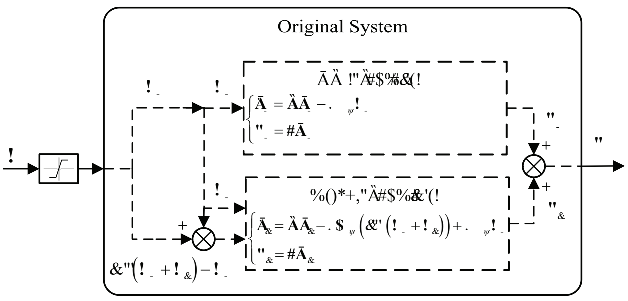

Fig. 2. Relationship of the original system and the two subsystems

The results of ASD for the original system (5) is shown in Fig. 2. The system input with saturation, $\mathrm{sat}(\mathbf{u})$, is seen as the sum of $\mathbf{u}_{\mathrm{p}}$ and $\mathrm{sat}(\mathbf{u}_{\mathrm{p}} + \mathbf{u}_{\mathrm{s}}) - \mathbf{u}_{\mathrm{p}}$. As a result, the primary system (7) is a linear system, and the secondary system (9) is a saturated nonlinear system.

Since both the primary system (7) and the secondary system (9) are virtual systems as shown in Fig. 2, an observer for $\mathbf{y}_{\mathrm{p},k}$ and $\mathbf{x}_{\mathrm{s},k}$ is necessary for controllers (10) and (14).

Theorem 3. Design an observer to obtain estimated values of $\mathbf{y}_{\mathrm{p}}$ and $\mathbf{x}_{\mathrm{s}}$ in system (7) and (9) as follows:

$$\text{Observer:} \begin{cases} \dot{\hat{\mathbf{x}}}_{\mathrm{s}} = \mathbf{A}\hat{\mathbf{x}}_{\mathrm{s}} - g\mathbf{G}_{\psi}\left(\mathrm{sat}\left(\mathbf{u}\right)\right) + g\mathbf{B}_{\psi}\mathbf{u}_{\mathrm{p}} \\ \hat{\mathbf{y}}_{\mathrm{p}} = \mathbf{y} - \mathbf{C}\hat{\mathbf{x}}_{\mathrm{s}}, \hat{\mathbf{x}}_{\mathrm{s}}(0) = \mathbf{0}. \end{cases} \tag{15}$$

Then, $\hat{\mathbf{y}}_{\mathrm{p}} \equiv \mathbf{y}_{\mathrm{p}}$ and $\hat{\mathbf{x}}_{\mathrm{s}} \equiv \mathbf{x}_{\mathrm{s}}$.

Proof. Subtracting equation (15) from the secondary system (9) results in $\dot{\tilde{\mathbf{x}}}_{\mathrm{s}} = \mathbf{A}\tilde{\mathbf{x}}_{\mathrm{s}}, \mathbf{x}_{\mathrm{s}}(0) = \mathbf{0}$, where $\tilde{\mathbf{x}}_{\mathrm{s}} = \mathbf{x}_{\mathrm{s}} - \hat{\mathbf{x}}_{\mathrm{s}}$. Then, one has $\tilde{\mathbf{x}}_{\mathrm{s}} \equiv \mathbf{0}$. Therefore, $\hat{\mathbf{y}}_{\mathrm{p}} \equiv \mathbf{y} - \mathbf{c}^{\mathrm{T}}\hat{\mathbf{x}}_{\mathrm{s}} \equiv \mathbf{y}_{\mathrm{p}}$. □

Remark 3. The two subsystems (7) and (9) obtained by ASD are the virtual systems. Therefore, the initial value of the original system can be assigned to the primary system (7), and the initial value of the secondary system (9) can be set to zero, i.e., $\mathbf{x}_{\mathrm{s}}(0) = \mathbf{0}$, $\mathbf{x}_{\mathrm{p}}(0) = \mathbf{x}_0$.

Based on the two subsystem controllers (10), (14), the observer (15), the final controller is obtained in the following theorem.

Theorem 4. Assume that *Problems 1-2* are solved for the original system (5), then, the final controller can be constructed as follows

$$\text{Observer:} \begin{cases} \dot{\hat{\mathbf{x}}}_{\mathrm{s},k} = \mathbf{A}\hat{\mathbf{x}}_{\mathrm{s},k} - g\mathbf{G}_{\psi}\left(\mathrm{sat}\left(\mathbf{u}\right)\right) + g\mathbf{B}_{\psi}\mathbf{u}_{\mathrm{p}} \\ \hat{\mathbf{y}}_{\mathrm{p},k} = \mathbf{y} - \mathbf{C}\hat{\mathbf{x}}_{\mathrm{s},k}, \hat{\mathbf{x}}_{\mathrm{s},k}(0) = \mathbf{0} \end{cases}$$

$$\text{Controller:} \begin{cases} \mathbf{u}_{k+1}(t) = \mathbf{u}_{\mathrm{p},k}(t) + \mathbf{\Gamma}_{\mathrm{d}}\dot{\hat{\mathbf{e}}}_{\mathrm{p},k}(t) \\ \qquad\qquad + \mathbf{L}\hat{\mathbf{x}}_{\mathrm{s},k+1}(t) \\ \mathbf{u}_1 = \mathbf{0} \end{cases} \tag{16}$$

where $\hat{\mathbf{e}}_{\mathrm{p},k} = \mathbf{y}_{\mathrm{d}} - \hat{\mathbf{y}}_{\mathrm{p},k}$. Then, the outputs of the original system (5) satisfy $\mathbf{y}_{\mathrm{d}} - \mathbf{y}_k \to \mathbf{0}$ as $k \to \infty$.

Proof. According to *Theorem 3*, observer (15) will make $\hat{\mathbf{x}}_{\mathrm{s}} \equiv \mathbf{x}_{\mathrm{s}}$, $\hat{\mathbf{y}}_{\mathrm{p}} \equiv \mathbf{y}_{\mathrm{p}}$, and $\hat{\mathbf{e}}_{\mathrm{p},k} \equiv \mathbf{e}_{\mathrm{p},k}$. First, we have

$$\begin{aligned} \|\mathbf{e}_k\|_{[0,T]} &= \|\mathbf{y}_{\mathrm{d}} - \mathbf{y}_k\|_{[0,T]} \\ &\le \|\mathbf{y}_{\mathrm{d}} - \mathbf{y}_{\mathrm{p},k}\|_{[0,T]} + \|\mathbf{y}_{\mathrm{s},k}\|_{[0,T]} \\ &= \|\mathbf{e}_{\mathrm{p},k}\|_{[0,T]} + \|\mathbf{e}_{\mathrm{s},k}\|_{[0,T]}. \end{aligned}$$

Then, according to *Theorem 1* and *Theorem 2*, we further have

i) if *Problem 1* is solved, controller (10) can guarantee $\|\mathbf{e}_{\mathrm{p},k}\|_{[0,T]} \to 0$ as $k \to \infty$ and

ii) if *Problem 2* is solved, controller (14) can guarantee $\|\mathbf{e}_{\mathrm{s},k}\|_{[0,T]} \to 0$ as $k \to \infty$.

Consequently, the final controller can guarantee $\|\mathbf{e}_k\|_{[0,T]} \to 0$, that is $\|\mathbf{y}_{\mathrm{d}} - \mathbf{y}_k\|_{[0,T]} \to 0$ as $k \to \infty$. □

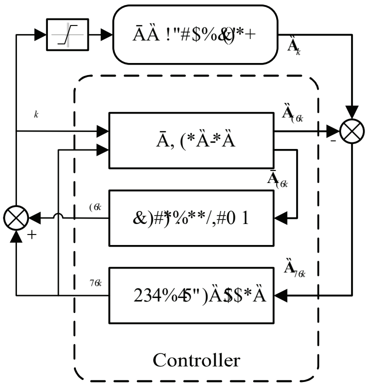

Fig. 3. The final controller structure for the original system (5)

The closed-loop system structure with controller (16) and observer (15) is shown in Fig. 3. In this paper, observer (15) is regarded as a part of the final controller. According to $\mathbf{y}_s$ from observer (15) and $\mathbf{y}$ from the original system (5), the ILC controller for the primary system (7) produces the control instruction $\mathbf{u}_{p,k}$ for the present iterative control process. The state feedback for the secondary system (9) generates the real-time control command $\mathbf{u}_s$ by $\mathbf{x}_s$ from observer (15).

4 Simulation

Simulation results are shown to demonstrate the effectiveness of the final controller designed before in this section.

4.1 Parameter Setting

Consider the original system (5) and the observer (15) with the following parameters:

$$\mathbf{u}_{\min} = \begin{bmatrix} -0.023 \\ -0.033 \end{bmatrix}, \mathbf{u}_{\max} = \begin{bmatrix} 0.041 \\ 0.021 \end{bmatrix}.$$

The desired trajectory is selected as

$$\mathbf{p}_{\mathrm{hd}}(t) = \begin{bmatrix} \frac{1}{10}(\cos(t) - 1)^2 \\ \frac{1}{10}\sin(t)t \end{bmatrix}$$

where $T = 3\mathrm{s}$, $\mathbf{v}_{\mathrm{hd}}(t) = \dot{\mathbf{p}}_{\mathrm{hd}}(t)$.

The controller is designed as equation (16) with the following parameters:

$$\mathbf{L} = \begin{bmatrix} 1 & 0 & 0 & 0 \\ 0 & 1 & 0 & 0 \end{bmatrix}, \mathbf{\Gamma}_{\mathrm{d}} = -\frac{1}{g}\begin{bmatrix} 1 & 0 \\ 0 & -1 \end{bmatrix}$$

where $g = 9.81\mathrm{m/s}^2$. In this simulation, set the yaw angle $\psi = 0$.

Note that

$$\mathbf{e}_k = \begin{bmatrix} e_1 \\ e_2 \end{bmatrix}, \mathbf{e}_{\mathrm{p},k} = \begin{bmatrix} e_{\mathrm{p}1} \\ e_{\mathrm{p}2} \end{bmatrix}.$$

4.2 Simulation Results

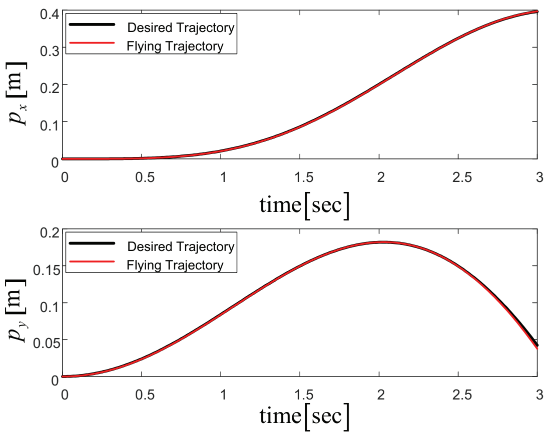

Fig. 4. Flying trajectory with ILC

Fig. 4 indicates that the multicopter flies along the desired trajectory under controller (16) designed before. Finally, the system inputs do not exceed the input saturation as shown in Fig. 5. Figs. 6,7 respectively show the primary system outputs and the secondary system outputs. Note that the primary system outputs and the secondary system outputs in Figs. 6,7 comprise the velocity values and the position values. Since the last several iteration results are similar, only the first few iteration results and the last iteration results are shown in Figs. 5,6,7. Figs. 8,9,10 indicate that the output errors of system (5), system (7), and system (9) all converge to zero as $k \to \infty$. Concretely, the outputs of the primary system track the desired trajectory and the secondary system output errors converges to zero, i.e., the outputs of the original system converges to the desired trajectory. The simulation results give the evidence of the feasibility and effectiveness

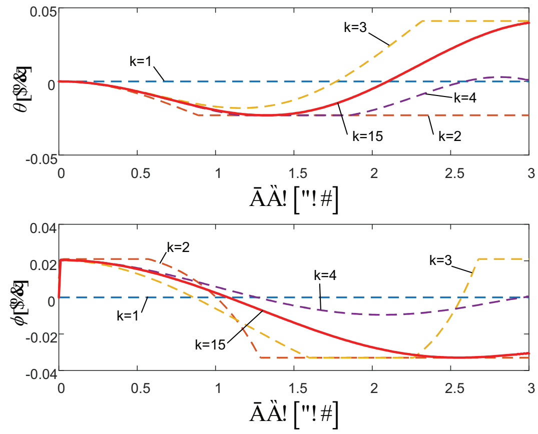

Fig. 5. System input with saturation

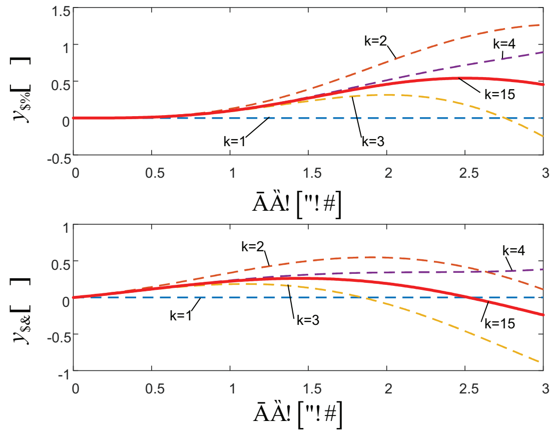

Fig. 6. The primary system output

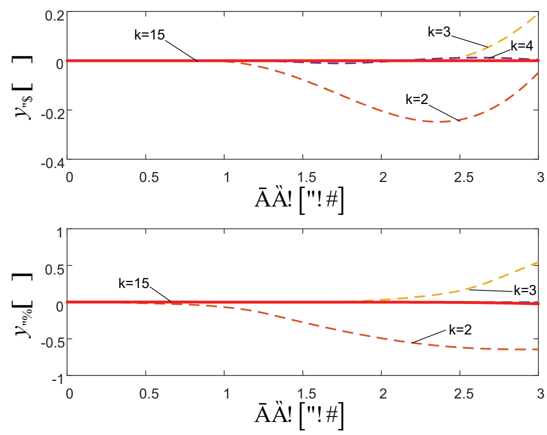

Fig. 7. The secondary system output

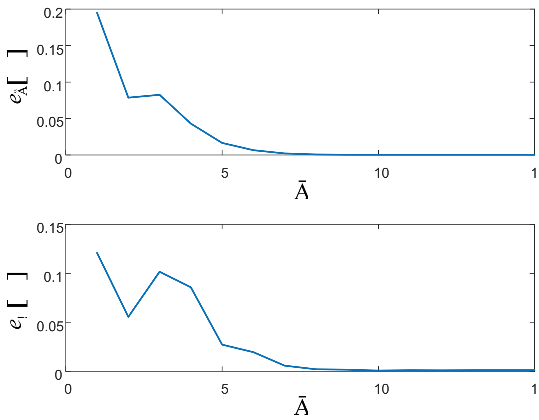

Fig. 8. Output error of the original system (5)

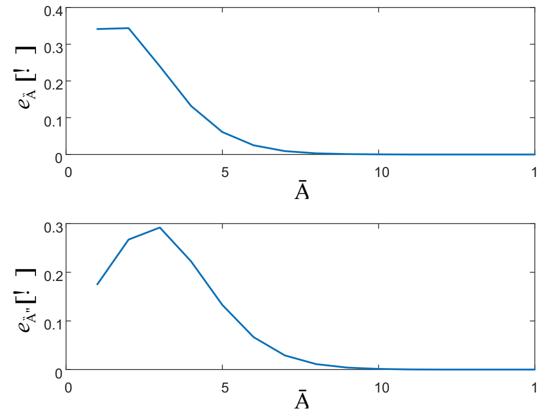

Fig. 9. Output error of the primary system (7)

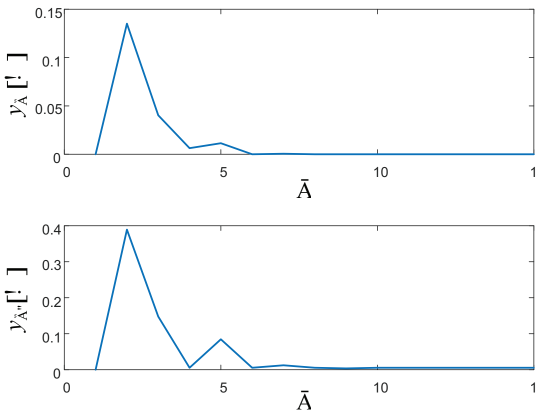

Fig. 10. Output error of the secondary system (9)

of the ASD method for the saturated ILC trajectory tracking problem of multicopters with input saturation.

5 Conclusions

The saturated ILC trajectory tracking problem for the multicopter horizontal channel is solved by applying the ASD method, in this paper. First, the multicopter horizontal channel model with a nonlinear term is given. Since the output matrix does not satisfy the convergence condition of the D-type ILC method, the velocity of the multicopter is added to the position of the multicopter to establish a new output. Then, by applying the ASD method, the D-type ILC controller can be designed for the primary system (7), and the state feedback is applied to the nonlinear secondary system (9). Comparing with classical linearization methods, the process of ASD based method is clear without ignoring any nonlinear elements. What is more, the ASD method simplifies the final controller.

References

[1] D. Bristow, M. Tharayil, and A. Alleyne, A survey of iterative learning control, *IEEE Control Systems*, 26(3): 96–114, 2006.

[2] S. Arimoto, S. Kawamura, and F. Miyazaki, Bettering operation of robots by learning, *Journal of Field Robotics*, 1(2): 123–140, 1984.

[3] Y. Chen, and K. Moore, A practical iterative learning path-following control of an omni-directional vehicle, 4(1): 90–98, 2002.

[4] O. Purwin, and R. D' Andrea, Performing aggressive maneuvers using iterative learning control, in *IEEE International Conference on Robotics and Automation*, 2009: 1731–1736.

[5] R. Longman, Iterative learning control and repetitive control for engineering practice, *International Journal of Control*, 73(10): 930–954, 2000.

[6] Q. Quan and K.-Y. Cai, Additive decomposition and its applications to internal-model-based tracking, in *Proceedings of 48th IEEE Conference on Decision and Control*, 2009, 817–822.

[7] Q. Quan, K.-Y. Cai, and H. Lin, Additive-state-decomposition-based tracking control framework for a class of nonminimum phase systems with measurable nonlinearities and unknown disturbances, *International Journal of Robust and Nonlinear Control*, 25(2): 163–178, 2015.

[8] T. Sogo, K. Kinoshita, and N. Adachi, Iterative learning control using adjoint systems for nonlinear non-minimum phase systems, in *Proceedings of 39th IEEE Conference on Decision and Control*, 2000, 3445–3446.

[9] G.-M. Jeong, and C. Choi, Iterative learning control for linear discrete time nonminimum phase systems, *Automatica*, 38(2): 287–291, 2002.

[10] Z.-B. Wei, Q. Quan, and K.-Y. Cai, Output feedback ILC for a class of nonminimum phase nonlinear systems with input saturation: an additive-state-decomposition-based method, *IEEE Transactions on Automatic Control*, 62(1): 502–508, 2017.

[11] Q. Quan, *Introduction to Multicopter Design and Control*. Springer, 2017.

[12] N. Amann, D. Owens, and E. Rogers, Iterative learning control for discrete-time systems with exponential rate of convergence, in *IEE Proceedings-Control Theory and Applications*, 1996, 217–224.

[13] M. Sun, and D. Wang, Iterative learning control with initial rectifying action, *Automatica*, 38(7): 1177–1182, 2002.

[14] M. Sun, and B. Huang, *Iterative Learning Control*. Chinese: National Defense Industry Press, 1999.